Melatonin Ameliorates Axonal Hypomyelination of Periventricular White Matter by Transforming A1 to A2 Astrocyte via JAK2/STAT3 Pathway in Neonatal Rats Induced by Lipopolysaccharide Injection

Shuqi Jiang
Guangdong Provincial People's Hospital
Huifang Wang
Guangdong Provincial People's Hospital
Qiuping Zhou
Guangdong Provincial People's Hospital
Qian Li
Guangdong Provincial People's Hospital
Nan Liu
Guangdong Provincial People's Hospital
Zhenggong Li
Guangdong Provincial People's Hospital
Chunbo Chen
Guangdong Provincial People's Hospital
yiyu deng (yiyudeng666@163.com)
Guangdong Provincial People's Hospital https://orcid.org/0000-0002-0459-7399

Research

Keywords: astrocyte, sepsis, melatonin, hypomyelination, neuroprotection

Posted Date: August 31st, 2021

DOI: https://doi.org/10.21203/rs.3.rs-841144/v1

Abstract

Background: Astrocyte A1/A2 phenotypes may play differential role in the pathogenesis of periventricular white matter (PWM) damage in septic postnatal rats. In this study, we sought to determine whether melatonin(MEL) would improve the axonal hypomyelination and neurological dysfunction, and, if so, to ascertain whether this may be related to transformation of astrocyte A1 to A2 phenotype.

Methods: One-day-old Sprague–Dawley rats were divided into control, LPS, and LPS+MEL groups. Immunofluorescence was performed to detect IBA1, GFAP, MAG, C3 and S100A10 in the PWM of neonatal rats. C1q, IL-1α and TNF-α expression were assessed by immunofluorescence and ELISA. Electron microscopy was conducted to observe alterations of axonal myelin sheath in the PWM, and the number of PLP and MBP positive oligdendrocytes was caculated using in situ hybridization. The effects of MEL on locomotor ability, spatial learning and memory were evaluated by behavioral testing. *In vitro*, A1 astrocyte was induced by IL-1α, C1q and TNF-α, the effect of MEL on C3 and S100A10 expression was determined by Western blot and immunofluorescence. JAK2/STAT3 signaling pathway was investigated to determine whether it was involved in modulation of A1/A2 phenotype transformation.

Results: At 1 and 3 days after LPS injection, $IBA1^+$ microglia in the PWM were significantly increased in cell numbers which generated excess amounts of IL-1α, TNF-α, and C1q. The number of A1 astrocytes was significantly increased at 7-28d after LPS injection. In rats given MEL treatment, the number of A1 astrocytes was significantly decreaed, but that of A2 astrocytes, PLP^+, MBP^+ and MAG^+ cells was increased. By electron microscopy, ultrastructural features of axonal hypomyelination were attenuated by MEL. Furthermore, MEL improved neurological dysfunction as evaluated by different neurological tests. *In vitro*, MEL decreased the C3 significantly, and upregulated expression of S100A10 in primary astrocytes subjected to IL-1α, TNF-α and C1q treatment. Additionally, JAK2/STAT3 signaling pathway was found to be involved in modulation of A1/A2 phenotype transformation.

Conclusions: MEL effectively alleviates PWMD of septic neonatal rats, and that it is most likely through modulating astrocyte phenotypic transformation from A1 to A2 via the MT1/JAK2/STAT3 pathway.

Introduction

Neonatal sepsis is the cause of substantial morbidity and mortality in the newborns resulting in adverse neurodevelopmental outcomes including cerebral palsy, retinopathy of prematurity, sensorineural hearing loss and cognitive defects[1–4]. A hallmark pathological feature is cerebral white matter injury, particularly periventricular white matter (PWM) damage (PWMD)[5,6]. We reported previously that PWMD induced by neonatal sepsis was associated with microglial activation, diffuse reactive astrogliosis, loss of oligodendrocyte progenitor cells (OPCs) and resultant hypomyelination[7–9].Microglia and astrocytes are resident glial cell types of the central nervous system (CNS), known to produce key inflammatory mediators following infection with pathogens[10,11]. It has been reported that microglia are the main source of inflammatory factors in the early stage of neuroinflammatory response, while astrocytes play an

important role in the later stage of chronic inflammatory response[12]. There is increasing evidence that astrogliosis may lead to the developmental impairment of the CNS[13–17]. Astrocytes provide trophic support for neurons, regulate the generation of new blood vessels, promote formation and function of synapses, and are involved in a wide range of homeostatic maintenance functions[18–20]. However, in response to noxious stimulation and nerve injury, astrocytes can undergo a series of phenotypic and functional changes and transform into reactive astrocytes[21]. Recent studies have shown that neuroinflammation and ischemia induced two different types of reactive astrocytes, referred to as “A1” and “A2”[13]. It has been reported that lipopolysaccharide (LPS)-activated microglia-conditioned medium or a composite of interleukin 1α (IL-1α), tumor necrosis factor α (TNF-α), and complement component 1q (C1q) can elicit A1 astrocytic activation in cultures. A1 phenotype has been shown to upregulate different classical complement cascade genes, and Complement 3 (C3) which is detrimental to neurons and oligodendrocytes. On the other hand, A2 phenotype, induced by ischemia, upregulates many neurotrophic factors, which foster survival and growth of neurons. A2 also produces S100A10 that promotes cell proliferation and membrane repair[13,22].

Melatonin is a key neurohormone that is beneficial for many neurological disorders including Alzheimer’s disease[23], Parkinson’s disease[24], Huntington’s disease[25], amyotrophic lateral sclerosis[26,27], and multiple sclerosis[28]. Melatonin as well as its metabolites are endowed with diverse pharmacological properties such as anti-inflammatory, anti-oxidative and anti-apoptotic effects. Melatonin exerts its effects through its cognate receptor, namely, melatonin receptor 1A (MT1), localized in different types of cells in the CNS including the neurons, microglia and astrocytes[29–31]. Moreover, the indoleamine exhibits a protective role against neurological disorders through inhibiting astrocyte activation. Previous studies have shown that melatonin effectively inhibited Aβ protein induced-astrocyte activation, reduced neuroinflammation and attenuated neurodegeneration and memory impairment. More recently, it has been shown that melatonin prevented astrocyte activation in a newborn mouse model of hypoxic-ischemic brain injury[34]. We reported previously that activated astrocytes were closely associated with PWMD induced by neonatal sepsis[35]. Given its anti-inflammatory and anti-oxidative properties, it would be therefore of great interest to explore if melatonin would help repair the PWMD in septic neonatal brain. Along with this, it would also be relevant to ascertain if melatonin would transform A1 to A2 phenotype in the PWM of septic neonatal brain and, if so, to determine if this might coincide with attenuation of axonal hypomyelination and improvement of neurological dysfunction. Addtionally, we sought to investigate whether melatonin would regulate transfomation of A1 to A2 phenotypic via the MT1/JAK2/STAT3 pathway. The present results suggest that melatonin indeed may serve as a potential therapeutic agent to attenuate PWMD induced by the bacterial toxin LPS by promoting astrocyte polarization from A1 to A2 phenotupe that is neuroprotective.

Materials And Methods

Animals and treatments

One-day-old Sprague–Dawley (SD) rats were purchased from the Laboratory Animal Center of Sun Yat-sen University (Guangzhou, China). All rats were kept in a facility with a 12-hour light/dark cycle (light on 9:00 a.m.-9:00 p.m.). The rats at postnatal day 1 (P1) were randomly assigned to three groups: (1) control group (Control), (2) LPS injection group (LPS), and (3) LPS + Melatonin injection group (LPS + MEL). Rats in the LPS group received a single intraperitoneal injection of LPS (1 mg/kg) derived from *Escherichia coli* O111:B4 (Sigma-Aldrich, L4391), while the control group was intraperitoneally administered with 0.01M phosphate buffered saline (PBS) (1 mg/kg). The rats in the LPS + MEL group were injected intraperitoneally with melatonin (Sigma-Aldrich, MO, USA; catalogue number: M5250) (10 mg/kg) at 7d after LPS injection (1 mg/kg) and, thereafter, once daily until postnatal day 28. The rats in each group were sacrificed at different time points at 1, 3, 7 ,14, and 28 days. The number of rats in each group is given in Table 1. All animal experimental procedures were approved by the Institutional Animal Care and Use Committee, Guangdong Province, China. The experimental design can be seen in Supporting Fig. 1.

Table 1
Number of rats killed at various time points after the LPS intraperitoneal injection (inside the round brackets) or LPS + MEL treatment (inside the square brackets) and their age-matched controls for different experiments (outside the brackets).

Age	Immunofluorescence	In situ hybridization	Electron microscopy	Open field test	Morris water maze test
1d	3(3)	/	/	/	/
3d	3(3)	/	/	/	/
7d	3(3)	/	/	/	/
14d	3 (3) [3]	3 (3) [3]	/	/	/
28d	3 (3) [3]	3 (3) [3]	3 (3) [3]	10 (10) [10]	10 (10) [10]

Open field test

Locomotor activity of rats was measured using an open field test (OFT) at 28d after LPS/melatonin injection. Rats were individually placed in a 75 cm × 75 cm open arena with 50 cm high walls and an infrared beam detection system. They were delivered to the testing room and allowed to leave from their home cages for 30 min before the test. Individual rats were placed in the center of the bright open field arena followed by recording of the locomotor behavior for a 5 min test session. The arena was cleaned with 70% ethanol between trials. The parameters of the total distance traveled, distances in the central area, and locomotor speed were recorded accordingly.

Morris water maze test

The rats were subjected to the Morris water maze test for spatial learning and memory assessment. The maze was a circular pool with 200 cm diameter and 30 cm height and filled with 25°C ± 1°C water. The pool was divided into four quadrants and remained the same along with the surrounding environment

throughout the test. A hidden square platform (10 cm in diameter) was located at 1 cm below the water surface in the center of target quadrant. In the acquisition trails, rats were placed into the pool to allow them find the hidden platform within 120 s. In the subsequent four days, the rats were trained to locate the platform at a fixed time each day, once per day. The rats released into the water with their heads up and facing the tank wall. The time taken for the rats to reach the fixed platform was recorded as the escape latency. To measure spatial memory for the previous platform location, the probe trials in which the platform was removed from the pool were performed in 24 h after the last learning trial. We recorded the relative times that rats crossed the original platform position within 120 s.

Primary astrocyte cultures and treatment

Primary cortical astrocyte cultures were prepared using 1-day-old neonatal SD rats (obtained from Laboratory Animal Center, Sun Yat-sen University, Guangdong Province, China). The adherent meninges were removed with a pair of fine forceps by using a dissecting microscope. Cells were counted using Scepter automated cell counter (JIMBIO FIL). Mixed glial cells separated from the cerebral cortex were plated on a 75 cm^2 flask at a density of 1.2x 10^6 cells/mL in Dulbecco's modified Eagle's medium/F12 medium (DMEM/F12, Gibco) supplemented with 10% fetal bovine serum (FBS) (Hyclone, Logan, UT). The mixed cells were cultured for 8–9 days in a humidified 5% CO_2 incubator at 37°C, and half of the medium was replaced about every 3–4 days. After 9–10 days, the flasks were shaken at room temperature at 180 rpm for 1 h to remove the microglial cells. After this, the flasks were added fresh DMEM/F12/FBS and continued to shake at 250 rpm for 18–20 h to ensure that OPCs were removed. Following this, purified astrocytes cultures subjected to different treatments were divided into different groups. A1 astrocytes were derived from primary purified astrocytes treated for 24 h with IL-1α (3 ng/ml, Sigma, I3901), TNF-α (30 ng/ml, Cell Signaling Technology, 8902SF), and C1q (400 ng/ml, MyBioSource, MBS143105). For the combination treatment, astrocytes were pretreated with melatonin (1 mM) for 1 h and then incubated with medium containing IL-1α, TNF-α and C1q for 24h incubation. Luzindole (100 μM) (the blocker of both MT1 and MT2 melatonin membrane receptors, abcam, ab145232) was added at 1 h prior to melatonin treatment. AG490 (10 μM) (the blocker of JAK2, MCE, CAS No.133550-30-5) and STAT-IN-3 (10 μM) (the blocker of STAT3, MCE, CAS No.2361304-26-7) were used along with melatonin to detect their effects on A1 astrocytes.

Double immunofluorescence

Rats from each time point in LPS group, LPS + melatonin group and their corresponding control group were deeply anesthetized with 4% pentobarbital. Under deep anesthesia, the rats were perfused transcardially first with PBS, followed 4% paraformaldehyde in 0.1 M phosphate buffer. Brains were removed and further fixed in 4% paraformaldehyde in 0.1 M phosphate buffer overnight at 4℃. After this, the brains were kept in 30% sucrose until use. Coronal frozen sections were cut at 10-μm thickness, and mounted on glass slides. Brain sections were obtained from different time points of three separate rat groups, namely, LPS group, LPS + melatonin group as well as their aged matching control group. The sections were processed for different treatments: Group I: brain sections were from each of the above-mentioned three rat groups sacrificed at 1, 3 and 7 days after LPS injection and their aged matching

controls. They were incubated with GFAP antibody. Group II: the brain sections were from rats in each group sacrificed at 1, 3 and 7 days after LPS injection and their aged matching controls. They were incubated with IBA1 antibody and IL-1α or TNF-α or C1q antibody. Group Ⅲ: the brain sections came from rats in each group sacrificed at 7, 14 and 28 days after LPS injection, LPS + melatonin injection and their aged matching controls. They were incubated with GFAP antibody and C3 or S100A10 antibody. Group IV: the brain sections were from rats in each group sacrificed at 14 and 28 days after LPS injection, LPS + MEL injection and their aged matching controls. They were incubated with antibody directed against anti-MAG. All the brain sections incubated with the respective primary antibodies (Table 2) were carried out overnight at 4℃. After washing three times by PBS, the sections were incubated at room temperature for 1h with appropriate fluorescent secondary antibodies: Alexa Fluor 488 Goat Anti-Chicken IgY (1:300, ab150169), Alexa Fluor 488 Goat Anti- Rabbit IgG (1:300, ab150077), Alexa Fluor 594 Goat Anti-Mouse IgG (1:300, ab150116), Alexa Fluor 594 Goat Anti-Rabbit IgG (1:300, ab150080). After three washes with PBS, DAPI (Sigma-Aldrich, D9542) was used for counterstaining of the nucleus and then viewed using a fluorescence microscope.

Table 2
Primary antibodies used in experiments

Antibody	Host	Company	Cat.NO.	Application (concentration)
GFAP	Chicken	Abcam	ab4674	IF (1:200)
IBA1	Rabbit	Abcam	ab178846	IF (1:200)
C1q	Mouse	Abcam	ab71940	IF (1:50)
IL-1α	Mouse	Abcam	ab239517	IF (1:100)
TNF-α	Mouse	Novus	NBP2-34301	IF (1:100)
C3	Rabbit	Abcam	ab200999	WB (1:1000)/IF (1:100)
S100A10	Rabbit	Thermo Fisher Scientific	PA5-95505	WB (1:1000)/IF (1:100)
MAG	Rabbit	Abcam	ab277524	IF (1:200)
GAPDH	Rabbit	Abcam	ab9485	WB (1:2000)
MT1	Rabbit	Novus	NBP1-28912	WB (1:1000)
JAK2	Rabbit	Abcam	ab108596	WB (1:1000)
P-JAK2	Rabbit	Abcam	ab32101	WB (1:1000)
STAT3	Rabbit	Abcam	ab68153	WB (1:1000)
P-STAT3	Rabbit	Abcam	ab76315	WB (1:1000)

The cultured spheres of primary astrocytes were treated with PBS or IL-1α, TNF-α and C1q or IL-1α, TNF-α, C1q and melatonin for 24 h. After treatment, immunofluorescence staining was carried out in primary

astrocytes following standard protocol. Briefly, primary cultured astrocytes were rinsed in PBS for three times. Next, the cells were fixed in 4% paraformaldehyde for 30 min and then blocked in 1% BSA for 1 h. After this, the primary astrocytes were incubated with primary antibodies against GFAP and C3 or S100A10 (Table 2) overnight at 4°C. Next, the primary astrocytes were incubated with appropriate secondary fluorescent antibodies. Finally, the primary astrocytes were counterstained with DAPI. After staining, the brain sections or cells were observed and photographed using a fluorescence microscope. Quantitative analysis of cell numbers in the PWM was carried out through counting the labeled cells in four different microscopic fields, respectively, by a blinded observer. The cells with a green IBA1 labeling fluorescent cell body overlapping with red were counted as $IBA1^+$ $C1q^+$, $IBA1^+$ $TNF\text{-}\alpha^+$, $IBA1^+$ $IL\text{-}1\alpha^+$ positive cells. The cells with a green GFAP labeling fluorescent cell body overlapping with red were counted as $GFAP^+$ $C3^+$ and $GFAP^+$ $S100A10^+$ positive cells. Positive cell count was performed using the Image J software.

ELISA

The expression levels of IL-1α, TNF-α and C1q in the PWM obtained from P1, P3 and P7 rats were determined. Rats exposed to LPS at 1, 3, and 7 days (n = 3 at each time) and their corresponding controls (n = 3 at each time point) were anesthetized with 4% pentobarbital. Subsequently, the brain was removed and processed accordingly. Briefly, the PWM tissues (about 100mg) were homogenized by grinders in 0.1 M phosphate buffer. Samples of supernatants were analyzed using a commercially available ELISA kit according to the manufacturer's protocol. Analysis of optical density was performed in a multifunctional microplate reader.

Electron microscopy and G-ratio analysis

Transmission electron microscopy was performed as previously described[9]. Briefly, P28 rats from control, LPS injection group and LPS + melatonin injection group were flushed through the left ventricle with PBS, followed by perfusion with a mixed aldehyde fixative composed of 2% paraformaldehyde and 3% glutaraldehyde in 0.1 M phosphate buffer, $_P$H=7.2. After perfusion, blocks of PWM tissues (about 1-mm thick) were further processed using standard methods for transmission electron microscopy. Tissue blocks were postfixed in 1% osmium tetraoxide for 2 h, followed by dehydration and final embedding in Araldite mixture. Ultrathin sections double stained with uranyl acetate and lead citrate were examined using a transmission electron microscope (HITACHI, model:HT7700). Electron microscopic images were captured at 4000× magnification. Four non-overlapping electron microscope images were randomly selected from each group to analyze the number of myelinated axons; the axon + myelin diameter was measured and calibrated by Image J software. G-ratio of the myelinated axon was then calculated, that is, the ratio of the axon diameter to the axon plus the myelin sheath diameter.

In situ hybridization

In situ hybridization was carried out as previously described[7,9]. Briefly, coronal frozen brain sections (10-μm thick) from P14 and P28 rats were incubated with proteinase K (S3004, Dako, Carpinteria, CA, USA) for 10 min and then rinsed in distilled water in 96% ethanol and in isopropanol for 5 min each time. Following this, the brain sections were incubated with hybridization mixture composed of distilled water, saline sodium citrate (SSC) buffer, 50% formamide, 50% dextran sulfate, Denhardt's solution (D2532, Sigma-Aldrich, Saint Louis, MO, USA), herring sperm DNA and 3'-digoxigenin-conjugated probe (Courtesy of Prof. Hui Fu's lab). After binding of horseradish peroxidase (HRP)-labeled probes, brain sections were colored with chromogenic substrate and dehydrated with alcohol (2 min for 70% and 95%, separately) and mounted. The probe details of PLP and MBP were described in our previous study. PLP and MBP positive cells were identified under a laboratory bright-field microscope (Olympus System Microscope Model BX53, Olympus Company Pte, Tokyo, Japan) at 40x magnification. The number of MBP and PLP positive cells in the PWM was calculated by counting four randomly selected microscopic fields in sections obtained from each rat by a blinded observer.

Western blot analysis

A protein extraction kit (Best Bio, BB-3101-100T) was used to extract the proteins from primary cultured astrocytes with different treatments. The standard protocol as previously described[7,36]was used to detect the protein concentrations by BCA Protein Assay Kit (Thermo Scientific, 23250). Samples of supernatants containing 30 μg of total protein were collected and heated at 100°C for 10 min. These samples were separated by SDS-PAGE and then transferred to a 0.22 μm polyvinylidene fluoride membranes (Bio-Rad, USA). Then, the membranes were blocked in 5% nonfat dried milk in Tris-buffered saline containing 0.05% Tween 20 (TBST) [0.05%(v/v) Tween-20 in 20 mmol/L (mm) Tris-HCl buffer, pH 7.6, containing 137 mm sodium chloride] for 1 h at room temperature, and then incubated with primary antibodies listed in Table 2. After three rinses in TBST, the membranes were hybridized with the appropriate secondary antibodies, including anti-mouse IgG (1:3000, Cell Signaling Technology, 7076S) or anti-rabbit IgG (1:3000, Cell Signaling Technology, 7074S) for 1h at room temperature. The protein bands were visualized by chemiluminescence kit (Millipore, WBKLS0500) and images were created by Image Quant LAS 500 Imager (GE Healthcare Bio-Sciences AB). The optical density of the respective protein bands was quantified with image J software.

Real-time reverse transcription polymerase chain reaction (RT-PCR)

Total RNA was extracted form primary cultured astrocytes subjected to different treatments by using Trizol reagent (Thermo Fisher Scientific). One μg of RNA were reversely transcribed to detect leukemia inhibitory factor (LIF) and Fibroblast Growth Factor 2 (FGF2) levels using the 5×PrimeScript RT Master Mix Kit (RR036A, Takara, Japan). Subsequently, 1μl of complementary DNA solution was used for real-time PCR in a 10μl reaction mixture containing 5μl 2×SYBR Premi×E×TaqTM (RR820A, Takara, Japan). The results were normalized to GAPDH. All the experiments were performed in triplicates as per the manufacturer’s instructions. The primer sequences used for RT-PCR are given in Table 3.

Table 3
Real-time PCR primer sequences

Primer	Sequence (5'–3')
GAPDH Forward	GTGCCAGCCTCGTCTCATAG
GAPDH Reverse	AGAGAAGGCAGCCCTGGTAA
LIF Forward	TCAACTGGCTCAACTCAACG
LIF Reverse	ACCATCCGATACAGCTCGAC
FGF2 Forward	CGGCTGCGGCTTCTAAGTC
FGF2 Reverse	GCCCCGTTTTGGACTCGAGT

Statistical analysis

All the values are expressed as the mean ± standard error of measurement (SEM). Statistical analyses were performed with IBM SPSS 25.0 statistical Software. Different statistical methods were applied according to different types of data. The data in Fig. 1, 2A, 3 and 5A-D with time (days after LPS injection) and treatment groups (vehicle, LPS or melatonin) were analyzed using two-way ANOVA. The data in Fig. 4E were analyzed by two-way ANOVA with treatment groups and training day (repeated measurement) as the independent variables. The data in Fig. 2C-F, 4A-D, F, 5F-H, 6 and 7 were compared using one-way ANOVA. $P < 0.05$ was considered as statistical significance.

Results

Microglia and astrocyte activation in the PWM of septic neonatal rats

To investigate the role of microglia and astrocytes in the PWM of neonatal rats injected with LPS, we first examined the expression of IBA1 and GFAP in the white matter composed of parallel arrays of axons. IBA1 and GFAP expression was detected by immunofluorescence which showed that the number of $IBA1^+$ $DAPI^+$ cells was noticeably increased in PWM at 1 and 3 days following LPS injection when compared with the matching control (Fig. 1A, B). The area of the PWM analyzed is shown in Supporting Fig. 2A. Of note, there was no significant difference in the number of $IBA1^+$ $DAPI^+$ cells at 7 days after LPS treatment when compared with the control group (Fig. 1B). Cell count results showed that the number of $GFAP^+$ $DAPI^+$ cells was significantly increased at 3 days and remained relatively stable in the PWM at 7 days after LPS injection (Fig. 2A, B) in comparison with the control. Studies have shown that A1 astrocytes can be induced by multiple inflammatory factors derived from microglia including IL-1α, TNF-α and C1q[13,40]. To confirm the activation state of astrocytes in septic brain injury model, rats were euthanized at 1, 3 and 7 days after LPS injection. Following this, the concentration of IL-1α, TNF-α and C1q in the PWM was evaluated. As shown in Fig. 1D-F, the concentration of IL-1α, TNF-α and C1q was significantly higher in

the septic group than that in the corresponding control. By immunofluorescence labeling, vigorous IL-1α, TNF-α and C1q expression was detected in microglia(Fig. 1A, Supporting Fig. 3, 4). Because the increased IL-1α, TNF-α and C1q expression in the PWM after LPS injection was mainly localized in the activated microglia; it is suggested that when released into the ambient environment they had activated and accounted for the transformation of astrocytes to A1 phenotype in the PWM of septic neonatal rats. In this study, A1 astrocyte was identified by its classical marker C3. As expected, the number of $C3^+$ $GFAP^+$ fluorescent astrocytes in the PWM was significantly increased 7 days after LPS injection in comparison with the matching control (Fig. 2C, D). Additionally, S100A10, a representative fluorescence marker for A2 astrocyte, was significantly decreased after LPS injection (Fig. 2E, F).

Melatonin induced transformation of LPS-induced A1 to A2 astrocyte

To explore the effect of melatonin on astrocyte phenotype, septic neonatal rats were given melatonin treatment at 7 days after LPS injection. Double immunofluorescence showed an increase in number of $C3^+$ $GFAP^+$ fluorescent astrocytes in the PWM at 14 and 28 days after LPS injection when compared with the corresponding control. Remarkably, in rats receiving melatonin treatment simultaneously, the number of $C3^+$ $GFAP^+$ astrocytes in the PWM of septic neonatal rats was decreased (Fig. 3A, B). This suggests that melatonin can reduce the number of A1 astrocytes in the PWM in septic neuronal rats.

Studies have reported that A2 astrocytes can exert neuroprotective effect and tissue repair by secreting different trophic factors. Expression of S100A10, a marker for A2 astrocyte, was significantly decreased after LPS treatment but it was rescued by melatonin. Double immunofluorescence showed S100A10 antibody and GFAP colocalization in astrocyte in the PWM. As shown in Fig. 3C, D, $S100A10^+$ $GFAP^+$ cells were markedly decreased in the PWM at 14 and 28 days after LPS injection; however, the number of $S100A10^+$ $GFAP^+$ cells was markedly increased in the PWM of septic rats treated with melatonin. Taken together, the results indicate that melatonin can reduce the number of A1 astrocytes. Concurrent to this, the number of A2 astrocytes was increased in the PWM in septic neonatal rats.

Melatonin improved the long-term neurological dysfunction of septic neonatal rats

To further assess whether melatonin could improve the long-term neurological dysfunction of septic neonatal rats, the open field test (OFT) and Morris water maze (MWM) test were performed at 28d after LPS injection. As shown in Fig. 4A, B, there were no significant differences in the total distance moved as well as the average movement speed of rats in the CON, LPS and LPS + MEL groups in the open field experiment, indicating that there were no obvious motor defects of the rats in each group. However, LPS-injected rats spent a shorter duration and moved for a shorter distance in the center area than the control group; whereas the duration of movement in the center area and the ratio between the distance in the center area and the total distance of the LPS + MEL group were significantly increased compared to that

of the LPS group. Thus, these results suggest that melatonin can help recovery of the rats from anxiety-like behavior induced by LPS (Fig. 4C, D).

Morris water maze test was used to evaluate the learning and memory function of rats at 28d after LPS/melatonin injection. At 28d following LPS injection, a slow learning process was measured by the escape latency to find the fixed platform during the first 4 days. It was markedly prolonged in comparison with the control group. In LPS injected rats treated with melatonin, a significant reduction in latency time was observed (Fig. 4E). Additionally, on the 5th day during the space exploration, the frequency of original platform crossings in the LPS group was significantly decreased when compared with the control group. However, a significantly higher number of platform location crosses was observed in the melatonin group than in comparison with the LPS group (Fig. 4F). These results indicated that melatonin treatment can rescue cognitive defects of rats challenged with LPS.

Melatonin attenuated axonal hypomyelination in the PWM in LPS-induced septic neonatal rats

Liddelow et al. (2017) demonstrated that A1 astrocytes were able to slow the differentiation and prolifertation of oligodendrocyte precursor cells. To verify whether melatonin would reverse the long-term impairments in myelination caused by LPS, we next explored whether melatonin would improve hypomyelination in the PWM at 14 and 28 days. The expression of mature myelin sheath associated proteins including MAG, MBP and PLP in the PWM was examined. Immunofluorescence showed that MAG expression in the PWM was obviously reduced in postnatal rats at 14 and 28 days after LPS injection. Very strikingly, melatonin administration reversed the decreased expression of MAG protein (Fig. 5A). The number of MAG^+ oligodendrocytes was significantly decreased in the PWM in septic rats at 14 and 28 days after LPS injection in comparison with the control (Fig. 5A, B). The area of the PWM analyzed is shown in Supporting Fig. 2B. Melatonin reversed the reduction in number of MAG^+ oligodendrocytes (Fig. 5A, B). To further elucidate whether melatonin would improve axonal hypomyelination in the PWM induced by LPS, *in situ* hybridization with antisense riboprobes targeted at MBP and PLP was performed for cell enumeration of MBP^+ and PLP^+ OLs in the PWM. Results of cell count showed that the number of MBP^+ and PLP^+ OLs was significantly decreased in the PWM at 14 and 28 days after LPS injection, a feature that was reversed by melatonin in which the number of MBP^+ and PLP^+ OLs was significantly increased (Fig. 5C, D, E).

By electron microscopy, at 28 days after LPS injection, many axons in the PWM were denuded of myelin sheath. In the sectional profiles, the myelin sheath became thinner when compared with that in the corresponding controls (Fig. 5F). Melatonin treatment resulted in an increase in number of myelinated axons whose myelin sheath, in general, was thicker than those in the untreated rats (Fig. 5F). The G-ratio is defined as the ratio of the axon diameter to the total diameter of axon plus its myelin sheath, which provides a reliable measure of axonal myelination. The G-ratio was used to compare myelin sheath of myelinated axons in the PWM in different groups. The average G-ratio of the myelinated axons in the PWM in the LPS-injected rats was significantly increased compared with their corresponding control

group. Bar graph H showed G-ratio values became larger in different diameters ranging from 0.2 to 1.2 μm as measured in electron micrographs in LPS group in comparison with the controls (Fig. 5H). However, G-ratio value was reversed after melatonin treatment when compared with LPS injection (Fig. 5G, H). Thus, melatonin treatment ameliorated LPS-induced axonal hypomyelination.

Mechanism of melatonin in inducing A1/A2 astrocyte transformation

To determine the underlying mechanism of A1/A2 astrocyte transformation regulated by melatonin, primary astrocytes were co-stimulated by IL-1α, TNF-α and C1q. Western blot was used to detect the protein expression levels of A1 astrocytic marker C3, and A2 astrocytic marker, S100A10. As shown in Fig. 6A-B, the protein expression level of C3 was significantly upregulated at 24h after IL-1α, TNF-α and C1q treatment; meanwhile, the expression level of S100A10 was declined when compared with the control primary astrocytes (Fig. 6C, D). We next treated the astrocytes with melatonin at 24h after incubation with IL-1α, TNF-α and C1q. Interestingly, the elevation in C3 protein expression levels induced by IL-1α, TNF-α and C1q was significantly inhibited by melatonin. As opposed to this, the low level expression of S100A10 induced by IL-1α, TNF-α and C1q was markedly enhanced. Of note, the melatonin effect in transforming A1 to A2 phenotype was blocked by luzindole, a melatonin receptor inhibitor (Fig. 6). Taken together, the results suggest that melatonin can induce A1/A2 astrocytes transformation through its receptor MT1.

To further investigate the underlying molecular mechanism of melatonin, we next explored whether the JAK2/STAT3 signaling pathways might be involved in the transformation of A1/A2 astrocytes. Western blot analysis showed that p-JAK2 and p-STAT3 protein expression was significantly decreased after IL-1α, TNF-α and C1q treatment when compared with the control primary astrocytes. Remarkably, the protein expression level of p-JAK2 and p-STAT3 was significantly enhanced at 24h after melatonin co-treatment with IL-1α, TNF-α and C1q (Fig. 7A). The results suggest that the JAK2-STAT3 pathway is activated by melatonin which thence induces the transformation of A1 to A2 astrocyte phenotype. To further confirm this, we used AG490, a JAK2 inhibitor, and STAT-IN-3 (a STAT3 inhibitor) to treat the primary astrocytes. As expected, the effect of melatonin on transformation of A1 to A2 phenotype was abrogated by the two inhibitors (Fig. 7B, C). These results suggest that melatonin can induce A1/A2 astrocyte transformation and that it is via the activation of the JAK2/STAT3 signal pathway.

We next sought to determine whether melatonin administration would upregulate the expression of LIF and FGF2 in the astrocytes. Real time RT-PCR analysis showed a significant decrease in the mRNA expression level of LIF and FGF2 in the astrocytes treated with IL-1α, TNF-α and C1q (Fig. 7D). Melatonin increased the mRNA expression level of LIF and FGF2 significantly in primary astrocytes treated with IL-1α, TNF-α and C1q. The results showed that melatonin can exert neuroprotective effect through inducing the expression of some neurotrophic factors such as LIF and FGF2. Importantly, we have shown that this via modulating A1/A2 astrocyte transformation.

Discussion

It is well documented that systemic LPS injection may induce neuroinflammation in the CNS with generation of excessive inflammatory factors that can cause the brain injury, especially the PWMD[37]. We have previously reported that LPS-induced microglial activation is the main component of the immune response and plays a key role in the pathogenesis of PWMD in septic neonatal rats [7,38]. A multitude of inflammatory cytokines, such as TNF-α and IL-1β, are released by activated microglia. In a separate study, it has been reported that activated microglia can induce A1 reactive astrocytes by secreting IL-1α, TNF-α, and C1q; indeed, these cytokines together play a pivot role to induce A1 astrocytes[13]. We have shown here that the number of $IBA1^+$ microglia was significantly increased in the PWM at 1 and 3 days after LPS injection, but the microglial population remained relatively stable and was comparable to the control at 7 days. Meanwhile, activated IBA1 activated microglia in the PWM showed increased production of IL-1α, TNF-α, and C1q. Compared with the microgila, the number of $GFAP^+$ astrocytes remained relatively unchanged at 1d but was noticeably increased at 3 and 7 days following LPS injection. It is suggested that microglia derived IL-1α, TNF-α, and C1q secreted into the microenvironment after LPS injection would promote the activation of A1 astrocytes. A1 astrocytes appear to preponderate in different human neuroinflammatory and neurodegenerative diseases. For example, in Alzheimer's disease, A1 astrocytes make up a majority of astrocyte population in the prefrontal cortex, 60% of which were C3 positive and likely to aggravate neurodegeneration[13]. Double immunofluorescence staining has shown that the number of $C3^+$ $GFAP^+$ cells was significantly increased in the PWM at 7 days after LPS injection. It stands to reason therefore that microglia were activated and produced excess amounts of IL-1α, TNF-α, and C1q, which could induce A1 astrocytes in the PWM of neonatal rats after LPS injection. Recent studies have reported that A1 astrocytes may gain neurotoxic functions and attack neurons and mature differentiated oligodendrocytes[39–41]. A1 reactive astrocytes can exert harmful effects because they secrete inflammatory factors such as IL-1β, IL-6, IFN-γ, and TNF-α along with the classical complement cascade genes and some unknown toxic factors deleterious to oligodendrocyte precursor cell differentiation, resulting in learning and memory impairments[13,42]. By contrast, A2 astrocyte activation was induced by ischemia, and activated A2 astrocyte are described to produce an array of neurotrophic factors, which are, therefore, considered to be protective to neurons or oligodendrocytes[16]. As a corollary, preventing A1 formation, promoting A1 reversion, or increasing A2 astrocytic polarization would provide great potential for protection of neurological functions in LPS-induced white matter damage in the developing brain.

Melatonin, secreted by the pineal gland, effectively modulates the inflammatory mechanism. Thus, it has been considered an option of choice as an anti-inflammatory agent for treating neuroinflammation. It is well documented that inflammatory response is implicated in different brain diseases, including Alzheimer's disease[43], Huntington's disease[44], traumatic brain injury[45], amyotrophic lateral sclerosis[46] and septic brain injury[9]. We have shown previously that LPS induces an increase numbers of reactive astrocytes and activated microglia in neonatal rats [35].We showed that IL-1β derived from activated microglia at 1–3 days after LPS injection would induce reactive astrocytes over a prolonged duration

which ultimately leads to neurological dysfunction at later life[35]. An interesting feature emerged from the present results was that the number of reactive astrocytes was significantly increased in the PWM at 7 d after LPS injection, yet the microglial population remained relatively stable. This is in accord with our previous finding that microglia might contribute to the early phase of cytokine production, whereas astrocytes are implicated in the release of inflammatory mediators at a late phase in brain pathologies over a protracted period. In order to gain a better understanding of the underlying mechanism of melatonin on reactive astrocytes rather than activated microglia, the rats were injected intraperitoneally with melatonin at 7 days after LPS injection, and then once daily until postnatal day 28. As expected, we found that melatonin reduced the increased number of $C3^+$ $GFAP^+$ cells in the PWM of neonatal rats subjected to LPS. Conversely, the number of $S100A10^+$ $GFAP^+$ cells was increased. The results lend support to the notion that melatonin plays an important role in phenotype transformation of A1/A2 astrocytes. Liddelow et al[13] reported that A1 reactive astrocytes inhibited OPCs proliferation, differentiation and migration. It is widely accepted that promoting the differentiation of OPCs into mature oligodendrocytes may contribute to the improvement of axonal hypomyelination in septic neonatal rats[9,47,48]. In consideration of the above, it is reasonable to suggest that melatonin could promote the differentiation and maturation of OPCs through regulating the phenotypic polarization from A1 to A2 astrocyte phenotype.

To further confirm if melatonin would improve axonal hypomyelination in the PWM of neonatal rats after LPS injection, the number of mature oligodendrocytes (OLs) was analyzed. Immunofluorescence and *in situ* hybridization results showed that melatonin increased the number of MAG^+, MBP^+ and PLP^+ cells in the PWM of septic neonatal rats. Ultrastructural study further confirmed that myelinated axons in sectional profiles were common; also, the axonal myelin sheath appeared thicker in the PWM of septic neonatal rats at 28 days after melatonin injection when compared with the matching control. It is suggested therefore that melatonin can improve the axonal hypomyelination in the PWM caused by LPS. More importantly, we have shown that melatonin improved the cognitive function in neonatal sepsis rats by behavioral tests. Thus, in the open field test, melatonin increased the duration of movement in the center area as compared with LPS injected rats. Furthermore, septic neonatal rats treated with melatonin showed shorter escape latency and increased times of crossing the original platform location when compared with the LPS treated rat in the Morris water maze test. These results strongly support that melatonin is beneficial in improving neurological dysfunctions of septic neonatal rats.

We next extended our study *in vitro* to investigate, whether melatonin would regulate the A1/A2 astrocyte polarization. To address this issue, primary astrocytes were treated with IL-1α, TNF-α and C1q, melatonin and luzindole (melatonin receptor antagonist). The expression of C3 and S100A10 in different experimental cell groups was then followed. The expression of C3 was significantly increased in the primary astrocytes after IL-1α, TNF-α and C1q treatment; conversely, the expression of S100A10 was significantly reduced. On the other hand, melatonin downregulated the protein expression of C3 in the astrocytes treated with IL-1α, TNF-α and C1q, but upregulated that of S100A10. In light of this, it is suggested that that melatonin can modulate the phenotypic transformation of A1 astrocytes to A2.

Melatonin is known to act on two major subtypes of melatonin-receptor MT1 and MT2 localized in the brain cells including microglia, astrocytes, oligodendrocytes and neurons[49–51]. Here, we found that the expression level of MT1 protein in primary astrocytes was decreased after treatment with IL-1α, TNF-α and C1q, but it was obviously increased after melatonin treatment. Luzindole, an inhibitor of MT1, could reverse the decreased expression of C3 and the increased expression of S100A10 induced by melatonin in the astrocytes. It can be confidently concluded therefore that melatonin can promote astrocytic polarization towards the neuroprotective A2 phenotype through its receptor MT1.

The Janus kinase/signal transducer and activator of transcription (JAK/STAT) signaling pathways play an important role in physiopathological processes, such as cell proliferation, cell apoptosis, and immune response [52,53]. It has been reported that STAT3 inactivation is involved in the pathogenesis of AD[52,54], and disruption of STAT3 signaling in astrocyte decreases mitochondrial function and increases oxidative stress[55]. The present results have shown that the expression level of p-JAK2 and p-STAT3 proteins in primary astrocytes was decreased after IL-1α, TNF-α and C1q treatment, but it was significantly increased after melatonin treatment. To further explore whether JAK2/STAT3 pathway was implicated in the process of the A1/A2 phenotype transformation modulated by melatonin, astrocytes were pretreated with AG490 (an inhibitor of JAK2) and STAT-IN-3 (an inhibitor of STAT3). The results showed that the expression level of p-JAK2 and p-STAT3 proteins was decreased respectively. This indicates that the effects of melatonin on the expression of C3 and S100A10 was significantly reversed. All evidence gained from the present results had converged and strongly indicated that melatonin can exert its neuroprotective effect through phenotype transformation of A1 to A2 astrocytes via the JAK2/STAT3 pathway.

There is additional evidence that A2 astrocytes exert neuroprotective and tissue repair effects by secreting different trophic factors[56,57]. In this connection, we have shown that the mRNA expression of LIF and FGF2 was significantly decreased in primary astrocytes treated with IL-1α, TNF-α and C1q, but it was upregulated following melatonin treatment. LIF and FGF2 are known to improve OPCs differentiation, promote oligodendrocyte survival, maturation, myelination and remyelination in experimental models of demyelination[58–61]. The up-regulated expression of LIF and FGF2 further suggests that melatonin can help restore the disorder in differentiation and maturation of OPCs, and improve axonal hypomyelination in the PWM of septic postnatal rats through modulating the transformation of A1 to A2 astrocyte.

Conclusion

It is unequivocal from this study that melatonin can reduce the number of A1 astrocytes and increase the number of A2 astrocytes in the PWM of septic neonatal rats. In tandem with this, melatonin increases the number of MAG^+, MBP^+ and PLP^+ OLs. This was coupled with attenuation of axonal hypomyelination and improvement of neurobehavioral disorders. *In vitro*, melatonin modulates phenotypic transformation of A1/A2 astrocytes through the MT1/JAK2/STAT3 signaling pathway. On the basis of these results, it is

concluded that melatonin can attenuate the axonal hypomyelination in the PWM and improve neurological disturbances of septic rats. This is attributed to the phenotypical transformation of A1 to A2 astrocyte phenotype via the MT1/JAK2/STAT3 signaling pathway induced by melatonin (Fig. 8). All in all, the results suggest that melatonin is a potential pharmacotherapeutic agent for mitigation of PWMD in septic neonatal rats.

Abbreviations

PWM: Periventricular white matter; PWMD: Periventricular white matter damage; A1: A classically activated astrocytic phenotype 1; A2: An alternatively activated astrocytic phenotype 2; JAK2: Janus kinase 2; STAT3: signal transducer and activator of transcription; LPS:lipopolysaccharide; IBA1:IL-1α:interleukin 1 alpha; GFAP: Glial fibrillary acidic protein; TNF-α: tumor necrosis factor alpha; C1q: complement component 1q; PLP: Proteolipid; MBP: Myelin basic protein; MAG: Myelin associated glycoprotein; C3: Complement 3; S100A10: S100 Calcium Binding Protein A10; OPCs: Oligodendrocyte progenitor cells; CNS: Central nervous system; MEL: Melatonin; MT1: Melatonin receptor 1; Aβ: amyloid β-protein; OFT: open field test; DMEM: Dulbecco's modified eagle medium; FBS: Fetal bovine serum; BCA: Bicinchonininc acid; BSA: Bovine serum albumin; DAPI: 4'6-diamidino-2-phenylindole; TBS: Tris-buffered saline; TBST: Trisbuffered saline Tween-20;

Declarations

Ethics approval and consent to participate All animals used in this study were handled following the protocols of the Institutional Animal Care and Use Committee, Guangdong Province, China (Animal Certificate No.: SYXK2012-0081).

Consent to publication All authors consent for the publication of the manuscript.

Availability of data and materials All data generated or analyzed during this study are included in this published article.

Competing interests The authors declare no competing interests.

Funding This study was supported by National Natural Science Foundation of China (Grant numbers: 82072230), Natural Science Foundation of Guangdong Province (Grant number: 2019A1515010206), Guangzhou Municipal Science and Technology Project (Grant number: 202002030094) and High-level Hospital Construction Project (Grant number: DFJH201804).

Authors' Contributions Designed and conceived the experiments: Yiyu Deng. Performed the experiments and analyzed the data: Shuqi Jiang. Contributed materials/reagents/analysis tools: Shuqi Jiang, Huifang Wang. Wrote the paper: Shuqi Jiang, Yiyu Deng.

Acknowledgments The authors would like to thank and acknowledge the help and support of other laboratory members.

Compliance with ethical standards

Research involving Human Participants and/or Animals We confirm adherence to ethical guidelines and indicate ethical approvals. No human researches were involved in this study.

Informed consent Not applicable.

References

1. Jung, E., Romero, R., Yeo, L. *et al.* The fetal inflammatory response syndrome: the origins of a concept, pathophysiology, diagnosis, and obstetrical implications. *Seminars in fetal & neonatal medicine* **25**, 101146, doi:10.1016/j.siny.2020.101146 (2020).
2. Ahlin, K., Himmelmann, K., Hagberg, G. *et al.* Cerebral palsy and perinatal infection in children born at term. *Obstetrics and gynecology* **122**, 41-49, doi:10.1097/AOG.0b013e318297f37f (2013).
3. Ferreira, R. C., Mello, R. R. , Silva, K. S. Neonatal sepsis as a risk factor for neurodevelopmental changes in preterm infants with very low birth weight. *Jornal de pediatria* **90**, 293-299, doi:10.1016/j.jped.2013.09.006 (2014).
4. Mwaniki, M. K., Atieno, M., Lawn, J. E. *et al.* Long-term neurodevelopmental outcomes after intrauterine and neonatal insults: a systematic review. *Lancet* **379**, 445-452, doi:10.1016/s0140-6736(11)61577-8 (2012).
5. Hofer, N., Müller, W. , Resch, B. White matter damage and neonatal sepsis. *Acta paediatrica (Oslo, Norway : 1992)* **100**, e1; author reply e1-2, doi:10.1111/j.1651-2227.2011.02217.x (2011).
6. Zaghloul, N. , Ahmed, M. Pathophysiology of periventricular leukomalacia: What we learned from animal models. *Neural Regen Res* **12**, 1795-1796, doi:10.4103/1673-5374.219034 (2017).
7. Han, Q., Lin, Q., Huang, P. *et al.* Microglia-derived IL-1β contributes to axon development disorders and synaptic deficit through p38-MAPK signal pathway in septic neonatal rats. *J Neuroinflammation* **14**, 52, doi:10.1186/s12974-017-0805-x (2017).
8. Xie, D., Shen, F., He, S. *et al.* IL-1β induces hypomyelination in the periventricular white matter through inhibition of oligodendrocyte progenitor cell maturation via FYN/MEK/ERK signaling pathway in septic neonatal rats. *Glia* **64**, 583-602, doi:10.1002/glia.22950 (2016).
9. Huang, P., Zhou, Q., Lin, Q. *et al.* Complement C3a induces axonal hypomyelination in the periventricular white matter through activation of WNT/β-catenin signal pathway in septic neonatal rats experimentally induced by lipopolysaccharide. *Brain Pathol* **30**, 495-514, doi:10.1111/bpa.12798 (2020).
10. Jeffries, A. M. , Marriott, I. Cytosolic DNA Sensors and CNS Responses to Viral Pathogens. *Frontiers in cellular and infection microbiology* **10**, 576263, doi:10.3389/fcimb.2020.576263 (2020).

11. Rothhammer, V., Borucki, D. M., Tjon, E. C. *et al.* Microglial control of astrocytes in response to microbial metabolites. *Nature* **557**, 724-728, doi:10.1038/s41586-018-0119-x (2018).
12. Kirkley, K. S., Popichak, K. A., Afzali, M. F. *et al.* Microglia amplify inflammatory activation of astrocytes in manganese neurotoxicity. *J Neuroinflammation* **14**, 99, doi:10.1186/s12974-017-0871-0 (2017).
13. Liddelow, S. A., Guttenplan, K. A., Larke, L. E. C. *et al.* Neurotoxic reactive astrocytes are induced by activated microglia. *Nature* **541**, 481-487, doi:10.1038/nature21029 (2017).
14. Liddelow, S. A. , Barres, B. A. Reactive Astrocytes: Production, Function, and Therapeutic Potential. *Immunity* **46**, 957-967, doi:10.1016/j.immuni.2017.06.006 (2017).
15. Shulyatnikova, T. , Verkhratsky, A. Astroglia in Sepsis Associated Encephalopathy. *Neurochemical research* **45**, 83-99, doi:10.1007/s11064-019-02743-2 (2020).
16. Miyamoto, N., Magami, S., Inaba, T. *et al.* The effects of A1/A2 astrocytes on oligodendrocyte linage cells against white matter injury under prolonged cerebral hypoperfusion. *Glia*, doi:10.1002/glia.23814 (2020).
17. Zou, L.-H., Shi, Y.-J., He, H. *et al.* Effects of FGF2/FGFR1 Pathway on Expression of A1 Astrocytes After Infrasound Exposure. *Frontiers in neuroscience* **13**, doi:10.3389/fnins.2019.00429 (2019).
18. Sofroniew, M. V. , Vinters, H. V. Astrocytes: biology and pathology. *Acta neuropathologica* **119**, 7-35, doi:10.1007/s00401-009-0619-8 (2010).
19. Khakh, B. S. , Sofroniew, M. V. Diversity of astrocyte functions and phenotypes in neural circuits. *Nat Neurosci* **18**, 942-952, doi:10.1038/nn.4043 (2015).
20. Allen, N. J. , Eroglu, C. Cell Biology of Astrocyte-Synapse Interactions. *Neuron* **96**, 697-708, doi:10.1016/j.neuron.2017.09.056 (2017).
21. Cregg, J. M., DePaul, M. A., Filous, A. R. *et al.* Functional regeneration beyond the glial scar. *Exp Neurol* **253**, 197-207, doi:10.1016/j.expneurol.2013.12.024 (2014).
22. Fujita, A., Yamaguchi, H., Yamasaki, R. *et al.* Connexin 30 deficiency attenuates A2 astrocyte responses and induces severe neurodegeneration in a 1-methyl-4-phenyl-1,2,3,6-tetrahydropyridine hydrochloride Parkinson's disease animal model. *J Neuroinflammation* **15**, 227, doi:10.1186/s12974-018-1251-0 (2018).
23. Cardinali, D. P., Furio, A. M. , Brusco, L. I. Clinical aspects of melatonin intervention in Alzheimer's disease progression. *Curr Neuropharmacol* **8**, 218-227, doi:10.2174/157015910792246209 (2010).
24. Belaid, H., Adrien, J., Karachi, C. *et al.* Effect of melatonin on sleep disorders in a monkey model of Parkinson's disease. *Sleep medicine* **16**, 1245-1251, doi:10.1016/j.sleep.2015.06.018 (2015).
25. Wang, X., Sirianni, A., Pei, Z. *et al.* The melatonin MT1 receptor axis modulates mutant Huntingtin-mediated toxicity. *The Journal of neuroscience : the official journal of the Society for Neuroscience* **31**, 14496-14507, doi:10.1523/jneurosci.3059-11.2011 (2011).
26. Zhang, Y., Cook, A., Kim, J. *et al.* Melatonin inhibits the caspase-1/cytochrome c/caspase-3 cell death pathway, inhibits MT1 receptor loss and delays disease progression in a mouse model of

amyotrophic lateral sclerosis. *Neurobiol Dis* **55**, 26-35, doi:10.1016/j.nbd.2013.03.008 (2013).

27. Jacob, S., Poeggeler, B., Weishaupt, J. H. *et al.* Melatonin as a candidate compound for neuroprotection in amyotrophic lateral sclerosis (ALS): high tolerability of daily oral melatonin administration in ALS patients. *J Pineal Res* **33**, 186-187, doi:10.1034/j.1600-079x.2002.02943.x (2002).
28. López-González, A., Álvarez-Sánchez, N., Lardone, P. J. *et al.* Melatonin treatment improves primary progressive multiple sclerosis: a case report. *J Pineal Res* **58**, 173-177, doi:10.1111/jpi.12203 (2015).
29. Dubocovich, M. L. , Markowska, M. Functional MT1 and MT2 melatonin receptors in mammals. *Endocrine* **27**, 101-110, doi:10.1385/endo:27:2:101 (2005).
30. Cecon, E., Liu, L. , Jockers, R. Melatonin receptor structures shed new light on melatonin research. *J Pineal Res* **67**, e12606, doi:10.1111/jpi.12606 (2019).
31. Jockers, R., Delagrange, P., Dubocovich, M. L. *et al.* Update on melatonin receptors: IUPHAR Review 20. *British journal of pharmacology* **173**, 2702-2725, doi:10.1111/bph.13536 (2016).
32. Ionov, M., Burchell, V., Klajnert, B. *et al.* Mechanism of neuroprotection of melatonin against beta-amyloid neurotoxicity. *Neuroscience* **180**, 229-237, doi:10.1016/j.neuroscience.2011.02.045 (2011).
33. Ali, T., Badshah, H., Kim, T. H. *et al.* Melatonin attenuates D-galactose-induced memory impairment, neuroinflammation and neurodegeneration via RAGE/NF-K B/JNK signaling pathway in aging mouse model. *J Pineal Res* **58**, 71-85, doi:10.1111/jpi.12194 (2015).
34. Sinha, B., Wu, Q., Li, W. *et al.* Protection of melatonin in experimental models of newborn hypoxic-ischemic brain injury through MT1 receptor. *J Pineal Res* **64**, doi:10.1111/jpi.12443 (2018).
35. Lin, Q., Shen, F., Zhou, Q. *et al.* Interleukin-1beta Disturbs the Proliferation and Differentiation of Neural Precursor Cells in the Hippocampus via Activation of Notch Signaling in Postnatal Rats Exposed to Lipopolysaccharide. *ACS Chem Neurosci* **10**, 2560-2575, doi:10.1021/acschemneuro.9b00051 (2019).
36. Deng, Y., Lu, J., Sivakumar, V. *et al.* Amoeboid microglia in the periventricular white matter induce oligodendrocyte damage through expression of proinflammatory cytokines via MAP kinase signaling pathway in hypoxic neonatal rats. *Brain Pathol* **18**, 387-400, doi:10.1111/j.1750-3639.2008.00138.x (2008).
37. Alshaikh, B., Yusuf, K. , Sauve, R. Neurodevelopmental outcomes of very low birth weight infants with neonatal sepsis: systematic review and meta-analysis. *Journal of perinatology : official journal of the California Perinatal Association* **33**, 558-564, doi:10.1038/jp.2012.167 (2013).
38. Xie, D., Shen, F., He, S. *et al.* IL-1beta induces hypomyelination in the periventricular white matter through inhibition of oligodendrocyte progenitor cell maturation via FYN/MEK/ERK signaling pathway in septic neonatal rats. *Glia* **64**, 583-602, doi:10.1002/glia.22950 (2016).
39. Liddelow, S. A., Guttenplan, K. A. , Barres, B. A. What do reactive astrocytes (really) do? *Glia* **67**, E33-E33 (2019).
40. Hinkle, J. T., Dawson, V. L. , Dawson, T. M. The A1 astrocyte paradigm: New avenues for pharmacological intervention in neurodegeneration. *Movement Disorders* **34**, 959-969,

doi:10.1002/mds.27718 (2019).

41. Yun, S. P., Kam, T. I., Panicker, N. *et al.* Block of A1 astrocyte conversion by microglia is neuroprotective in models of Parkinson's disease. *Nat Med* **24**, 931-938, doi:10.1038/s41591-018-0051-5 (2018).
42. Zhang, H. Y., Wang, Y., He, Y. *et al.* A1 astrocytes contribute to murine depression-like behavior and cognitive dysfunction, which can be alleviated by IL-10 or fluorocitrate treatment. *J Neuroinflammation* **17**, 200, doi:10.1186/s12974-020-01871-9 (2020).
43. Calsolaro, V. , Edison, P. Neuroinflammation in Alzheimer's disease: Current evidence and future directions. *Alzheimer's & dementia : the journal of the Alzheimer's Association* **12**, 719-732, doi:10.1016/j.jalz.2016.02.010 (2016).
44. Subhramanyam, C. S., Wang, C., Hu, Q. *et al.* Microglia-mediated neuroinflammation in neurodegenerative diseases. *Seminars in cell & developmental biology* **94**, 112-120, doi:10.1016/j.semcdb.2019.05.004 (2019).
45. Simon, D. W., McGeachy, M. J., Bayır, H. *et al.* The far-reaching scope of neuroinflammation after traumatic brain injury. *Nature reviews. Neurology* **13**, 171-191, doi:10.1038/nrneurol.2017.13 (2017).
46. Beers, D. R. , Appel, S. H. Immune dysregulation in amyotrophic lateral sclerosis: mechanisms and emerging therapies. *The Lancet. Neurology* **18**, 211-220, doi:10.1016/s1474-4422(18)30394-6 (2019).
47. Coppolino, G. T., Marangon, D., Negri, C. *et al.* Differential local tissue permissiveness influences the final fate of GPR17-expressing oligodendrocyte precursors in two distinct models of demyelination. *Glia* **66**, 1118-1130, doi:10.1002/glia.23305 (2018).
48. Vieira, M. S., Santos, A. K., Vasconcellos, R. *et al.* Neural stem cell differentiation into mature neurons: Mechanisms of regulation and biotechnological applications. *Biotechnology advances* **36**, 1946-1970, doi:10.1016/j.biotechadv.2018.08.002 (2018).
49. Olivier, P., Fontaine, R. H., Loron, G. *et al.* Melatonin promotes oligodendroglial maturation of injured white matter in neonatal rats. *PLoS One* **4**, e7128, doi:10.1371/journal.pone.0007128 (2009).
50. Paulose, J. K., Peters, J. L., Karaganis, S. P. *et al.* Pineal melatonin acts as a circadian zeitgeber and growth factor in chick astrocytes. *J Pineal Res* **46**, 286-294, doi:10.1111/j.1600-079X.2008.00659.x (2009).
51. Xiang, J., Zhu, W., Yang, F. *et al.* Melatonin-induced ApoE expression in mouse astrocytes protects endothelial cells from OGD-R induced injuries. *Translational psychiatry* **10**, 181, doi:10.1038/s41398-020-00864-9 (2020).
52. hiba, T., Yamada, M. , Aiso, S. Targeting the JAK2/STAT3 axis in Alzheimer's disease. *Expert opinion on therapeutic targets* **13**, 1155-1167, doi:10.1517/14728220903213426 (2009).
53. Yang, Y., Duan, W., Jin, Z. *et al.* JAK2/STAT3 activation by melatonin attenuates the mitochondrial oxidative damage induced by myocardial ischemia/reperfusion injury. *J Pineal Res* **55**, 275-286, doi:10.1111/jpi.12070 (2013).

54. Chiba, T., Yamada, M., Sasabe, J. *et al.* Amyloid-beta causes memory impairment by disturbing the JAK2/STAT3 axis in hippocampal neurons. *Molecular psychiatry* **14**, 206-222, doi:10.1038/mp.2008.105 (2009).
55. Sarafian, T. A., Montes, C., Imura, T. *et al.* Disruption of astrocyte STAT3 signaling decreases mitochondrial function and increases oxidative stress in vitro. *PLoS One* **5**, e9532, doi:10.1371/journal.pone.0009532 (2010).
56. Su, Y., Chen, Z., Du, H. *et al.* Silencing miR-21 induces polarization of astrocytes to the A2 phenotype and improves the formation of synapses by targeting glypican 6 via the signal transducer and activator of transcription-3 pathway after acute ischemic spinal cord injury. *FASEB journal : official publication of the Federation of American Societies for Experimental Biology* **33**, 10859-10871, doi:10.1096/fj.201900743R (2019).
57. Li, T., Chen, X., Zhang, C. *et al.* An update on reactive astrocytes in chronic pain. *J Neuroinflammation* **16**, 140, doi:10.1186/s12974-019-1524-2 (2019).
58. Butzkueven, H., Zhang, J. G., Soilu-Hanninen, M. *et al.* LIF receptor signaling limits immune-mediated demyelination by enhancing oligodendrocyte survival. *Nat Med* **8**, 613-619, doi:10.1038/nm0602-613 (2002).
59. Kerr, B. J. , Patterson, P. H. Leukemia inhibitory factor promotes oligodendrocyte survival after spinal cord injury. *Glia* **51**, 73-79, doi:10.1002/glia.20177 (2005).
60. Laterza, C., Merlini, A., De Feo, D. *et al.* iPSC-derived neural precursors exert a neuroprotective role in immune-mediated demyelination via the secretion of LIF. *Nat Commun* **4**, 2597, doi:10.1038/ncomms3597 (2013).
61. Azim, K., Raineteau, O. , Butt, A. M. Intraventricular injection of FGF-2 promotes generation of oligodendrocyte-lineage cells in the postnatal and adult forebrain. *Glia* **60**, 1977-1990, doi:10.1002/glia.22413 (2012).

Figures

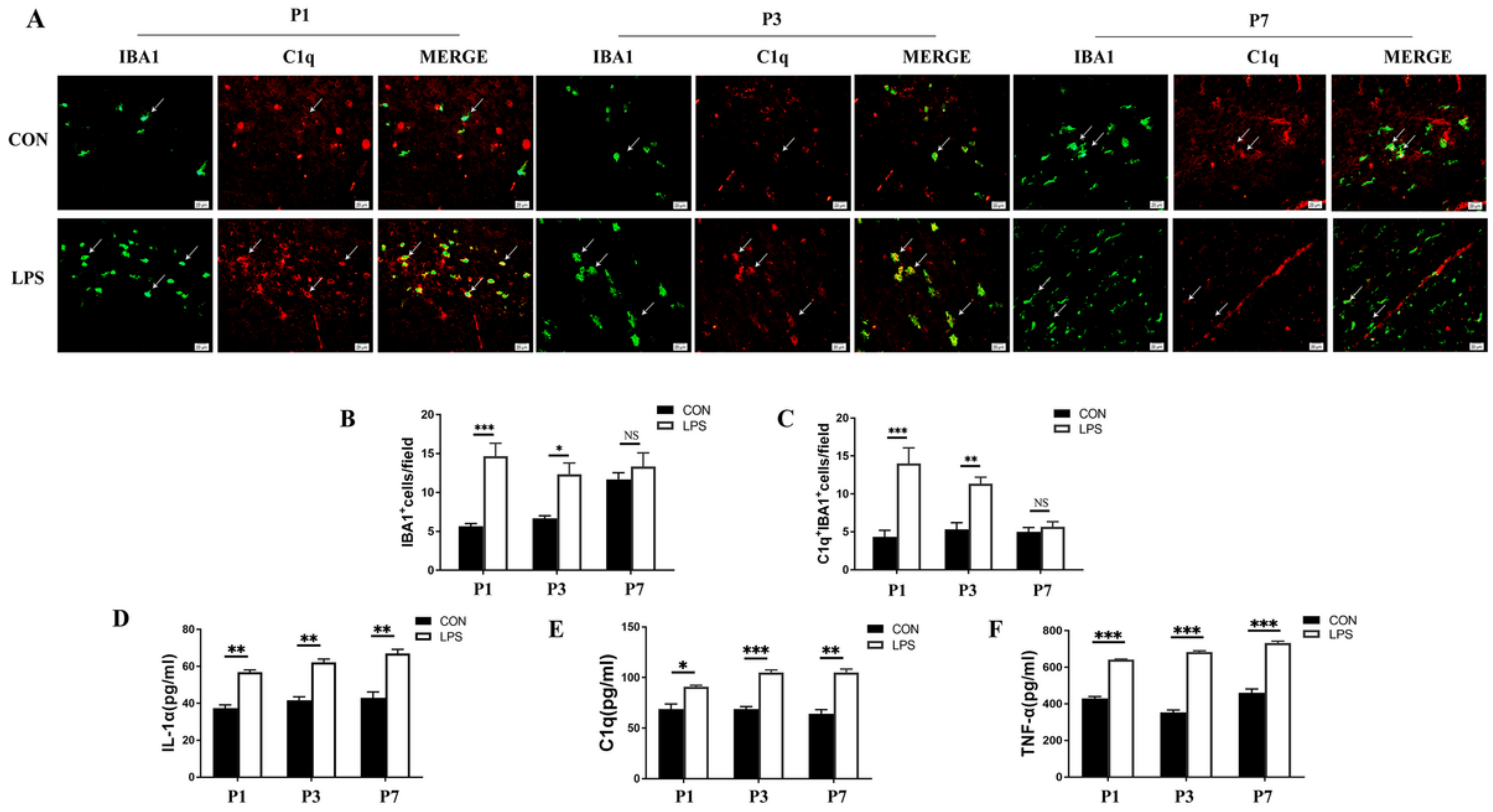

Figure 1

IL-1α, C1q and TNF-α protein expression in the PWM of postnatal rats at 1d, 3d and 7d after LPS injection and their matching controls. The number of IBA1+ cells was significantly increased at 1 and 3d after LPS injection, but the difference was not significant at 7d between LPS and control groups(A,B) (n=3 for each group).The co-localized expression of IBA1 and C1q in microglia could be seen in A. The number of C1q+ IBA1+ cells was significantly increased at 1 and 3d after LPS injection, but the difference was not significant at 7d between LPS and control groups(A, C), n=3 for each group. Quantification by Elisa shows significant increase in the cytokine secretion of IL-1α(D), C1q(E) and TNF-α (F) at 1, 3 and 7d after LPS exposure when compared with the corresponding control(n=3). Scale bars: 20μm. *P<0.05, **P<0.01, ***P<0.001.

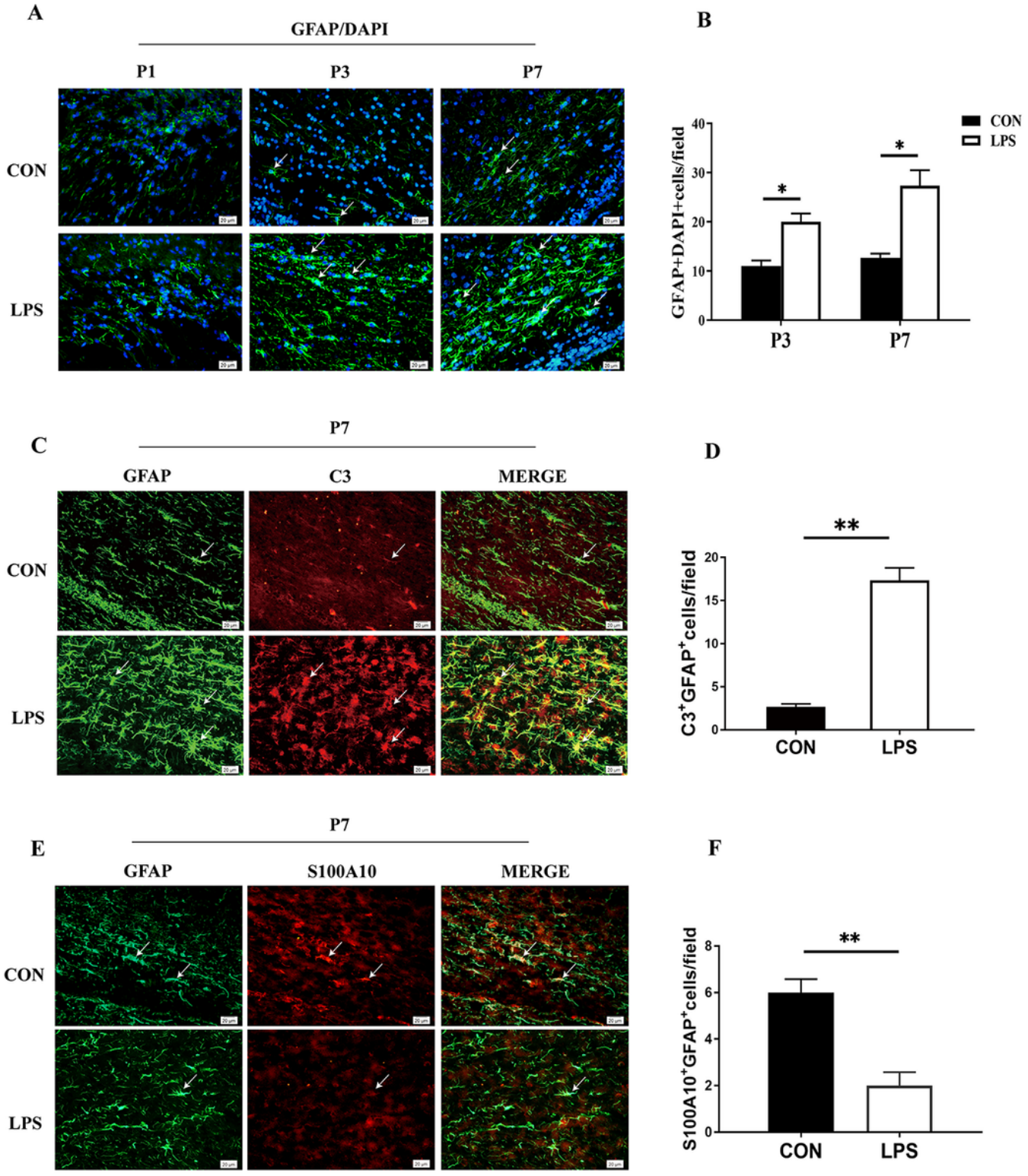

Figure 2

Immunofluorescence images of astrocytes in the PWM at 7 days after LPS injection and their matching controls. The astrocytes were labeled by anti-GFAP (green), and anti-C3 (red), and anti-S100A10 (red) for A1 and A2, respectively. The number of GFAP+ cells was significantly increased at 3 and 7d after LPS injection(A, B), (n=3 for each group). The number of C3+ GFAP+ cells was significantly increased at 7d after LPS injection(C), meanwhile, S100A10 expression in astrocytes at 7d was decreased after LPS

injection(E). Bar graph in D, F summarizes the frequency of C3+ GFAP+ cells and S100A10+ GFAP+ cells at 7d after LPS injection (n=3 for each group). Scale bars: 20μm. *P<0.05, **P<0.01.

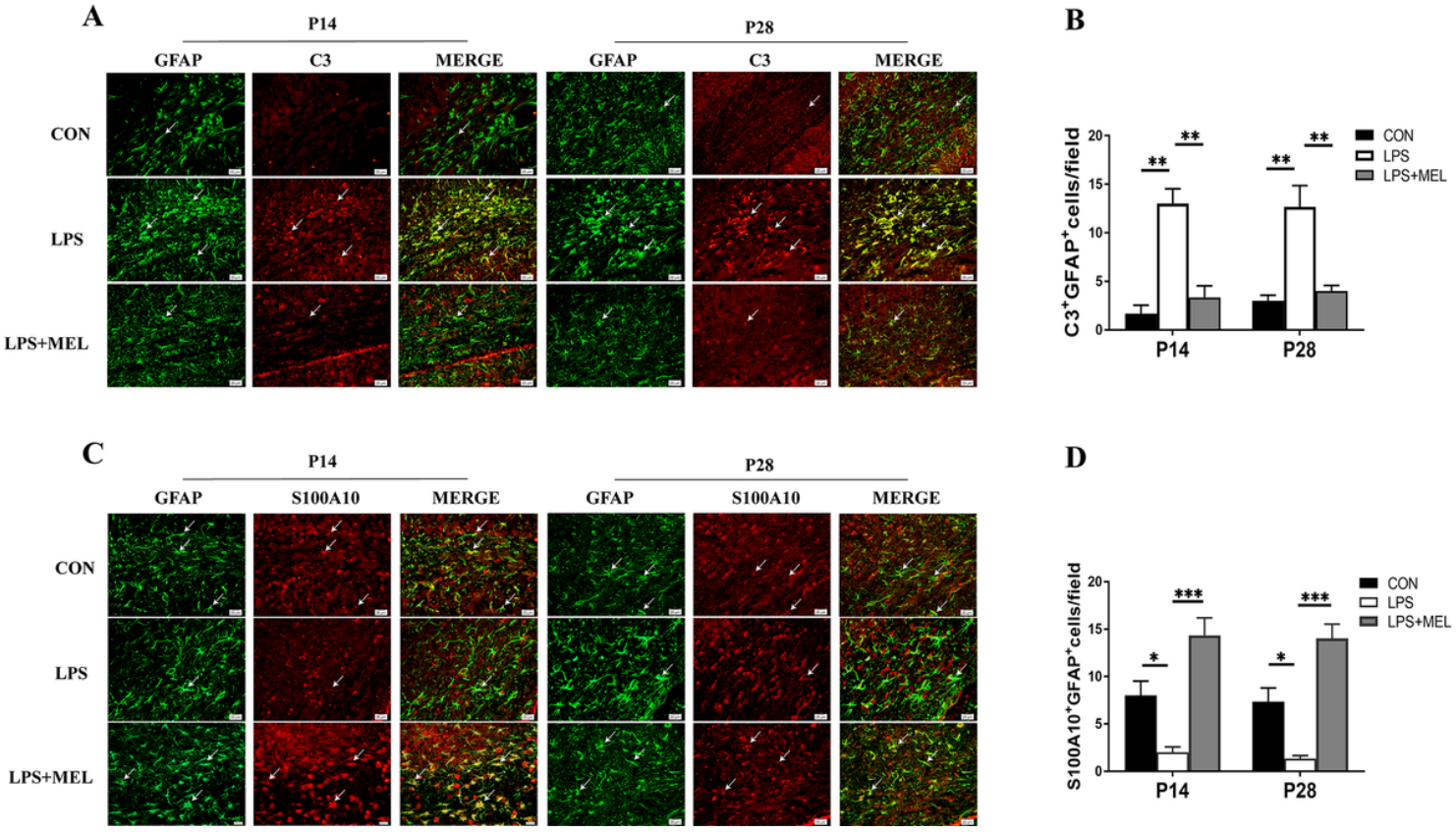

Figure 3

Melatonin counteracted LPS-induced A1/A2 astrocyte polarization in the PWM of septic neonatal rats. GFAP-labeled(green) and C3 (red) immunoreactive astrocytes are distributed in the PWM at 14 and 28d after LPS/melatonin injection and their corresponding controls. The number of C3+ GFAP+ cells was significantly increased at 14 and 28d after LPS injection compared with controls; however, it was significantly decreased after melatonin treatment (A, B) (n=3 for each group). GFAP-labeled(green) and S100A10 (red) immunoreactive astrocytes are distributed in the PWM at 14 and 28d after LPS/melatonin injection and their corresponding controls. Note the number of S100A10+ GFAP+ cells was significantly decreased at 14 and 28d after LPS injection compared with controls; however, it was significantly increased after melatonin treatment (C, D) (n=3 for each group). Scale bars: 20μm. *P<0.05, **P<0.01, ***P<0.001.

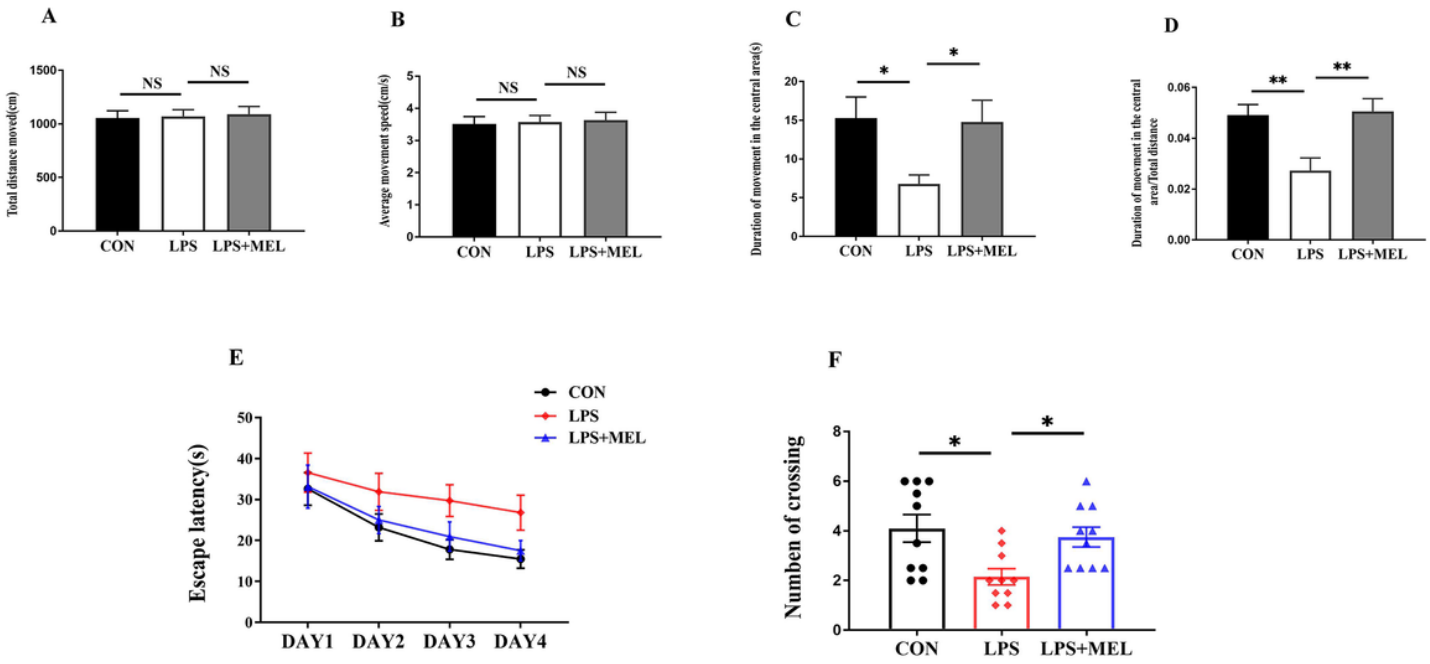

Figure 4

Melatonin improved anxiety behavior and spatial learning of rats given LPS injection. The effects of melatonin on behaviors in the open field test. In LPS + MEL group, the duration of movement in the central area (C) and the ratio between distance in the center area and the total distance (D) was increased compared with the LPS group. Melatonin treatment significantly improved spatial learning in Morris water maze test. Longer escape latencies and decreased number of times crossing the original platform location was observed in rats at 28 days after LPS injection when compared with control group; however, melatonin treatment significantly improved the impairment in cognitive deficits of rats after LPS injection as measured by shorter escape latencies and increased number of times crossing the original platform location(E,F). *P<0.05, **P<0.01. (n=10 for each group in every test).

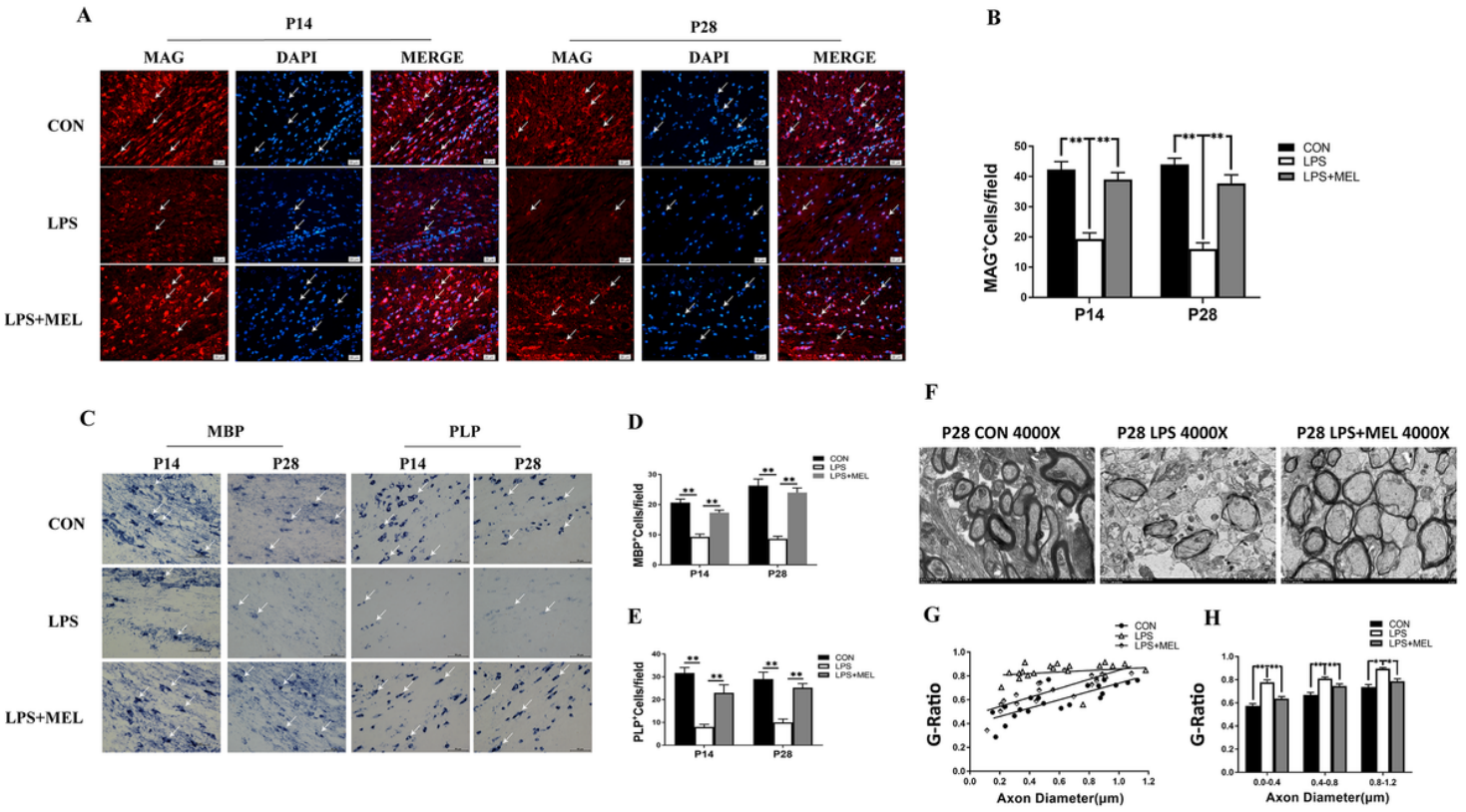

Figure 5

Melatonin attenuated axonal hypomyelination in the PWM in LPS-induced septic neonatal rats. MAG-labeled (red) and DAPI (blue) immunoreactive oligodendrocytes are distributed in the PWM at 14 and 28d after the LPS/melatonin injection and their corresponding controls. The number of MAG+ DAPI+ cells was significantly decreased at 14 and 28d after LPS injection compared with control; however it was significantly increased after melatonin treatment(A, B) (n=3 for each group; scale bars: 50μm). In situ hybridization shows the number of MBP+ and PLP+ oligodendrocytes was significantly decreased at 14 and 28d after LPS injection compared with controls; however, it was significantly increased after melatonin treatment(C-E), (n=3 for each group; scale bars: 50μm). Electron microscope images showing sectional profiles of myelinated axon in transverse section at the magnification of × 4000. The configuration of myelinated axons in the PWM of postnatal rats at 28 d after the LPS injection, LPS + MEL injection and their corresponding controls (F),(n=3 for each group; scale bars: 2 μm). Graph G showing G-ratio of myelinated axons of different diameters in the PWM at 28d after LPS injection and LPS + MEL injection and corresponding control. *P < 0.05, **P < 0.01.

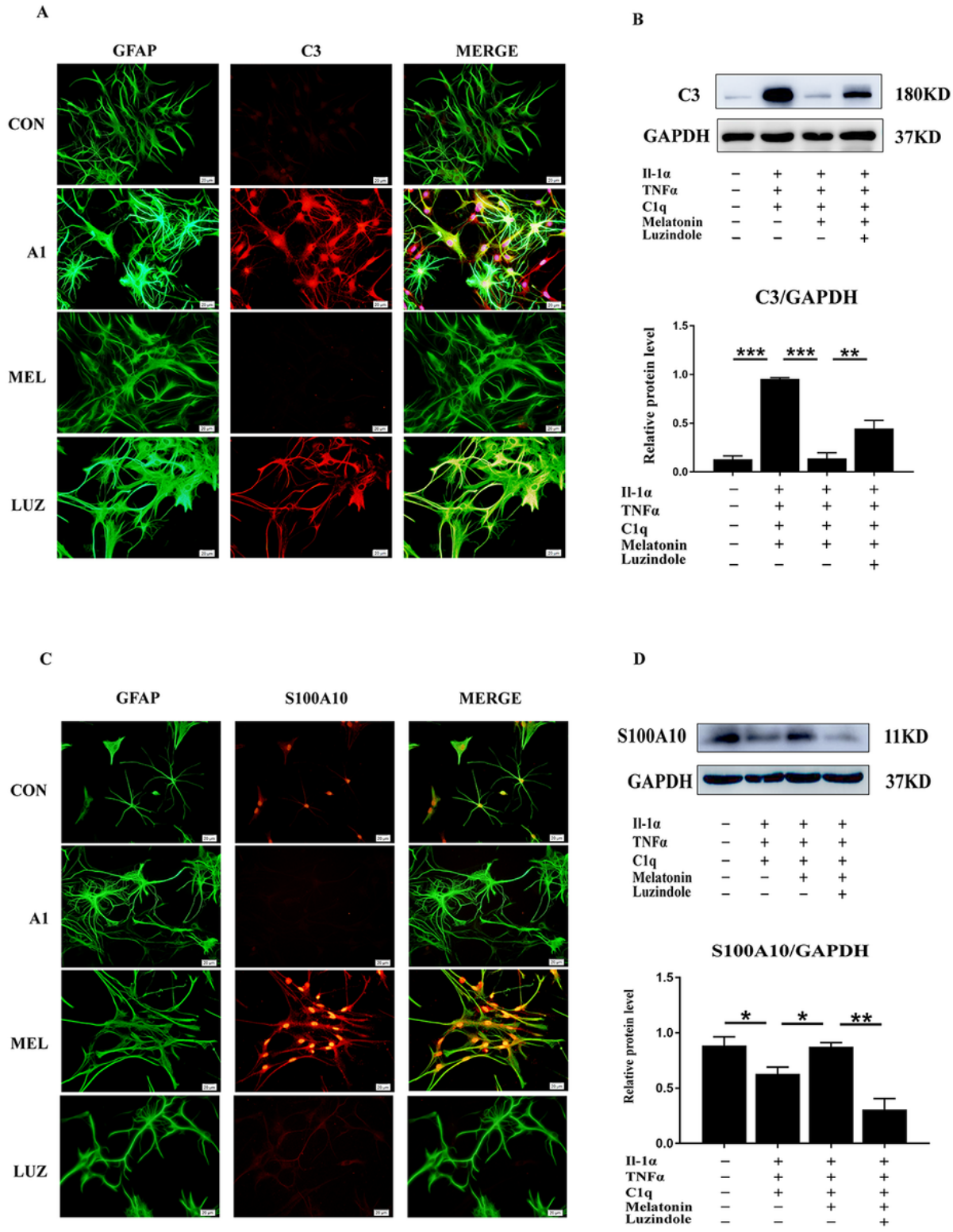

Figure 6

Melatonin reversed the increased expression of C3, and decreased expression of S100A10 in primary astrocytes stimulated by IL-1α, TNF-α and C1q in vitro. After melatonin treatment and IL-1α, TNF-α and C1q exposure, the astrocytes were processed for immunofluorescence staining using primary antibodies GFAP (green), and anti-C3 (red) for A1 detection. Immunofluorescence images of cultured primary astrocytes showing the expression of GFAP and C3 at 24h after the treatment with IL-1α + C1q + TNF-α,

IL-1α + C1q + TNF-α + melatonin and IL-1α + C1q + TNF-α + melatonin + luzindole when compared with the corresponding control(A). Panel B shows the optical density changes of C3 protein relative to GAPDH. A2 astrocytes were examined by immunofluorescence labeling using anti-GFAP (green) and A2 marker anti-S100A10 (red). Immunofluorescence images of cultured primary astrocytes showing expression of GFAP and S100A10 at 24h after treatment of IL-1α + C1q + TNF-α, IL-1α + C1q + TNF-α + melatonin, and IL-1α + C1q + TNF-α + luzindole when compared with the corresponding control(C). Panel D shows the optical density changes of S100A10 protein, relative to GAPDH. Scale bars: 20 μm. *P<0.05, **P<0.01, ***P<0.001 (n=3 for each group).

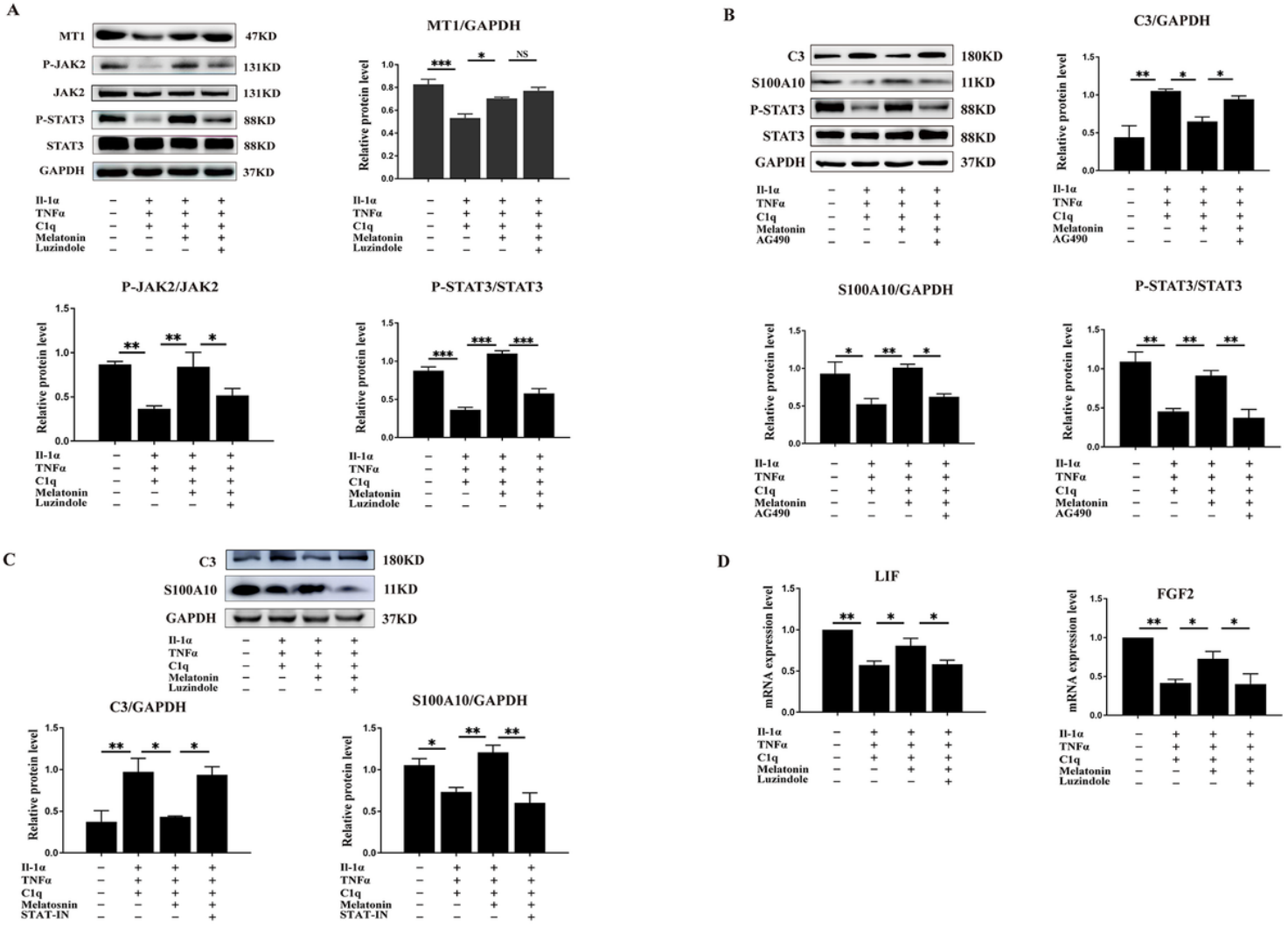

Figure 7

Melatonin activated MT1/JAK2/STAT3 pathway in primary astrocytes exposed to IL-1α, C1q and TNF-α in vitro. Panel A shows optical density changes of p-JAK2 relative to JAK2, p-STAT3 relative to STAT3 and MT1 relative to GAPDH in each group. IL-1α + C1q + TNF-α treatment for 24h significantly decreased the optical density of MT1, P-JAK2 and P-STAT3 proteins when compared with the corresponding controls. Melatonin reversed the changes, but the effect was prevented by luzindole. Additionally, blockage of JAK2 or STAT3 inhibited the effect of melatonin in modulating the A1/A2 astrocyte polarization. Panel B shows A1-marker C3, A2-marker S100A10, p-STAT3, STAT3 and GAPDH immunoreactive bands after IL-

1α + C1q + TNF-α, IL-1α + C1q + TNF-α + melatonin, and IL-1α + C1q + TNF-α + AG490(an inhibitor of JAK2 activity) treatment when compared with the corresponding control in primary astrocyte. Panel C show immunoreactive bands after IL-1α + C1q + TNF-α, IL-1α + C1q + TNF-α + melatonin, IL-1α + C1q + TNF-α + STAT-IN-3(an inhibitor of STAT3 activity) treatment when compared with the corresponding control in primary astrocyte. Note melatonin treatment activates MT1/JAK2/STAT3 pathway and then promoted A1 to A2 polarization. RT-qPCR shows mRNA expression changes in neurotrophic factors LIF and FGF2. GAPDH was used as the internal control. IL-1α + C1q + TNF-α treatment for 24h significantly decreased the mRNA expression of LIF and FGF2 when compared with the corresponding controls. Melatonin reversed the changes, but the effect of melatonin was prevented by luzindole (D). *P < 0.05, **P < 0.01 (n=3 for each group).

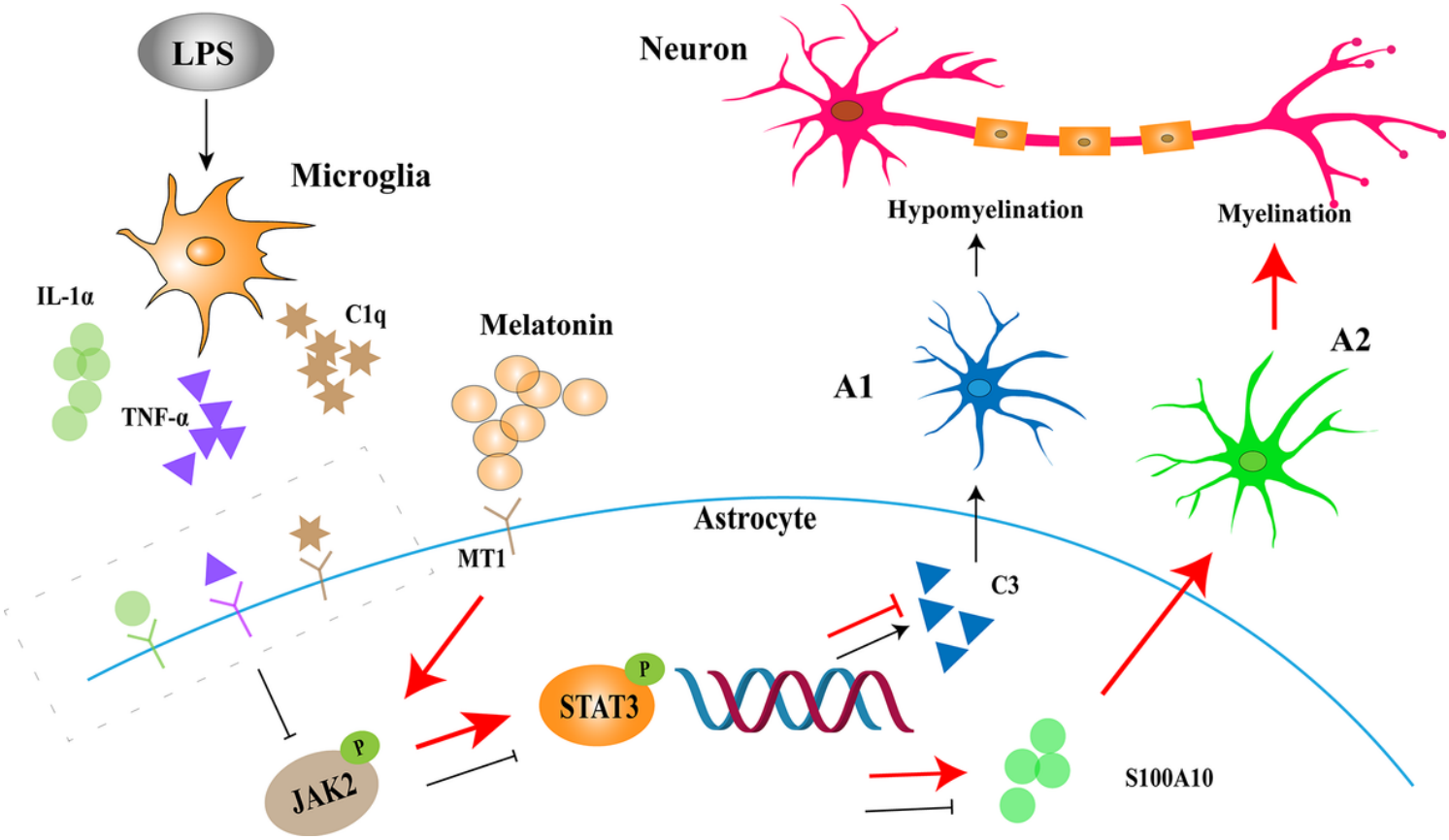

Figure 8

Table of Contents Image (TOCI): A schematic diagram depicting the cellular and molecular events associated with melatonin treatment in postnatal rats given LPS injection. Microglia are activated in the PWM after intraperitoneal injection of LPS and release massive amounts of IL-1α, TNF-α and C1q, which then induce A1 astrocyte activation. A1 astrocyte would contribute to axonal hypomyelination in the PWM in the septic neonatal rats. Melatonin binds to its cognate receptor (MT1) expressed on the astrocytes leading to activation of the JAK2/STAT3 pathways. This would decrease A1 astrocyte production of Complement 3, C3, and increase A2 astrocyte production of trophic factor, S100A10. Production of complement and neurotoxin by A1 astrocytes causes hypomyelination in the PWM after

LPS injection; on the other hand, production of trophic factors by A2 astrocytes induced by melatonin improves hypomyelination.

Supplementary Files

This is a list of supplementary files associated with this preprint. Click to download.

- SUR1.tif
- SUR2.tif
- SUR3.tif
- SUR4.tif